On the implementation of a hysteretic reactor model in EMTP

Sébastien Dennetière[1], Jean Mahseredjian[1] , Manuel Martinez[2], Michel Rioual[2], Alain Xémard[2], Patrick Bastard[3]

(1)IREQ / Hydro-Québec
1800 Lionel-Boulet
Varennes, Québec,
Canada, (jeanm@ireq.ca)

(2)Électricité de France
Direction des Études et Recherches
1 ave. du Général de Gaulle
92141 Clamart Cedex

(3)Supélec
Plateau de Moulon
3 Rue Joliot-Curie
91190 Gif-sur-Yvette Cédex, France

Abstract **– This paper presents the implementation of a hysteretic reactor model in a transient analysis package. The model is available in a currently developed EMTP (DCG-EPRI) version. It is demonstrated how the hysteretic reactor equations can be solved to eliminate topological limitations and allow solving large scale networks efficiently. Numerical robustness aspects and the representation of minor loops are emphasized. The model demonstrates new and not previously available computational capabilities.**

Keywords – Hysteresis, transients, nonlinearities, EMTP

I. INTRODUCTION

Magnetic hysteresis plays an important role in certain analysis cases associated with power systems. Practical examples are the inrush current and ferroresonance. The inclusion of a hysteresis branch in a transformer model allows representing residual flux effects and provides increased accuracy in the computation of losses. The challenge of an EMTP type model is to correctly simulate hysteresis with the inherent complexities related to minor loops.

The most commonly used hysteretic reactor model in EMTP is the pseudononlinear Type-96 model [1]. The pseudononlinear term implicates that the reactor is not solved simultaneously with the surrounding network equations. In addition to the well known limitations of such an approach, the Type-96 modeling assumptions make it a poorer candidate for matching experimental results.

In addition to this model, EMTP has recently introduced the Type-92 model [2]. This model is classified as a true-nonlinear model and therefore has the inherent ability to achieve a simultaneous solution with network equations. It remained however prone to numerical problems and limitations mainly due to the applied solution method for true-nonlinear models. Other aspects, such as the data fitting procedure, were using a less accurate method.

This paper starts by a summarized presentation on the limitations of the previously available EMTP models. It follows by the presentation of a new solution method for a physical model derived from [2][3]. Other details on the actual model are also provided.

The new implementation demonstrates unsurpassed capability for the simulation of large scale networks with hysteretic reactors located in arbitrary network configurations. A practical test case taken from the EDF (Electricité de France) system is shown to attain good numerical accuracy without degrading simulation performance.

II. PREVIOUS MODELS

The original EMTP Type-96 model is based on the theory developed in [4]. The hysteresis loops are modeled with piecewise linear approximations. Downward and upward trajectories are related by a translation on the x-axis and the minor loops are scaled in shape from the major loops. Some modifications have been proposed [5] to match experimental results. The model remained however unable to reproduce the experimental results presented in [3].

The minor loops trajectories of the Type-96 model were defined in terms of the major loop. In reality the minor loops have been shown to behave independently from the major loop trajectories. The Type-96 also assumed a single-valued characteristic for high currents.

In addition to physical modeling assumptions the Type-96 implementation was based only on the pseudo-nonlinear solution method of EMTP. This method converts the hysteresis slopes into a Norton equivalent which represents the relation between voltage and current at the given operating point and simulation time. Since there are no iterations it cannot be qualified as a simultaneous solution. The program changes operating segments only after illegally operating outside the range of the previous segment for one time-step. This results into the typical noisy behavior shown in Fig. 1. The integration time-step can be reduced to minimize such problems, but its drawback is a dramatically increased simulation time.

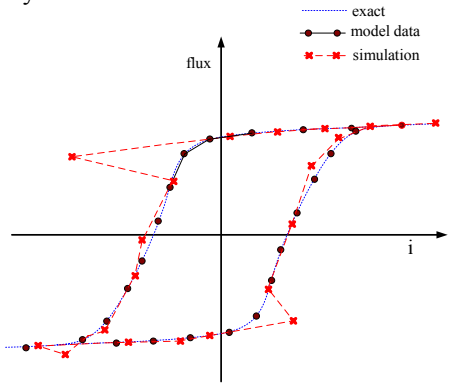

Fig. 1 A test case with the Type-96 model

The Type-92 model was based on the flux distortion view of saturation [3][6]. It has been programmed using the true-nonlinear compensation method [8] based solution technique of EMTP. This method can provide a simultane-

ous solution with network equations but imposes several significant topological and numerical limitations described in [9]. Among such limitations are the inability to include the hysteresis model with other nonlinear models in the same subnetwork and matrix singularity conditions.

III. The New Model

The hysteresis concept used by the new model is identical to the one proposed in [6]. The minor hysteresis loops are modeled using templates [3]. Each minor loop curve returns to the last reversal point from the current reversal point. The minor loops are closed upon exit and the trajectory is reverted back to the previous encompassing loop.

Some other details on the behavior of ferromagnetic material can be found in [7].

A. Modeling equations

Two separate functions are used. The first function is a hysteresis function relating 'unsaturated' flux λ_{unsat} to current. This function models the pure hysteresis effect. The second function is a saturation function relating instantaneous 'saturated flux' λ_{sat} to 'unsaturated' flux λ_{unsat}. This function represents the saturation effect. Both functions are geometrically represented by hyperbolic equations [2][10].

The saturation effect is given by:

$$C_{sat} = \left[\lambda_{unsat} - \frac{\lambda_{sat}}{S_{sv}} - X_{sv}\right]\left[S_{sh}\lambda_{unsat} - \lambda_{sat} + Y_{sh}\right] \quad (1)$$

The constant C_{sat} defines the curvature, it controls how close the curve is to its asymptotes. S_{sv} is the slope of the vertical asymptote, S_{sh} is the slope of the horizontal asymptote, X_{sv} is the x-axis intercept of the vertical asymptote and Y_{sh} is the y-axis intercept of the horizontal asymptote. Once the main shape of the saturation curve is defined, the concave function part is taken for positive values of λ_{unsat} and λ_{sat}. The relation between negative values is obtained by symmetry. The final saturation curve passes through the origin.

The relation between λ_{unsat} and current i is given by:

$$C_{hyst} = \left[i - \frac{\lambda_{unsat}}{S_{hv}} - X_{hv}\right]\left[S_{hh}i - \lambda_{unsat} - Y_{hh}\right] \quad (2)$$

The C_{hyst} defines the hysteresis effect curvature. The remaining variables are defined as in equation (1), but for the hysteresis effect. In this case the convex branch is chosen for the upward trajectory and the concave branch for the downward trajectory. Since it is needed to establish a closed shape, a movement of translation is performed on the asymptotes. Fig. 2 shows the initial curve (solid blue line) and the translated curve (red dashed line). The curves 1 and 2 form the hysteresis loop.

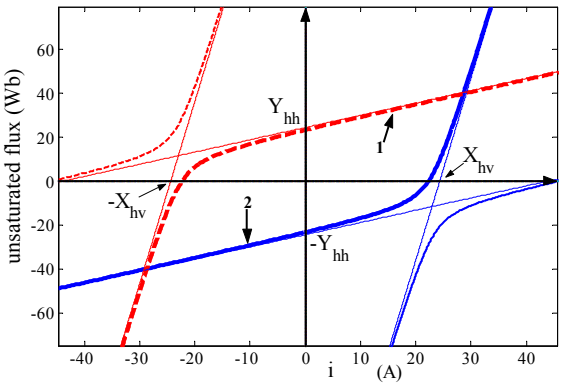

Fig. 2 Hysteresis modeling template

B. Hysteresis trajectories

Hysteresis trajectories follow a uniform template. Upward and downward trajectories correspond to opposite template orientations. The parameters X_{hv} and Y_{hh} control template position and are systematically modified during simulation. The parameters C_{hyst}, S_{hv} and S_{hh} are fixed and define template shape. Since template shape is independent of its position, the starting point for a trajectory (reversal point on the hysteresis loop) is chosen as the origin of the coordinate system. Then in accordance with the model, the vertical asymptote (slope S_{hv}) is displaced to the right (or to the left for downward trajectory) along the abscissa by a distance equal to twice the coercive current. A minor loop trajectory cannot exceed the major loop asymptote.

When a reversal point is detected, a new trajectory begins. A reversal point occurs when the flux $\phi(t+\Delta t) < \phi(t)$ on an upward trajectory or when $\phi(t+\Delta t) > \phi(t)$ on a downward trajectory. The reversal points preceding the current loop must be saved. Hyperbolic branches automatically pass through the previous to last reversal point. Fig. 3 illustrates the progression from the inner loop A. When the flux increases beyond the reversal point 5, the reversal point that defines the trajectory is 4. That is why a reversal point stack composed of (λ_{unsat}, i) value pairs is used to save the reversal points out of the present loop.

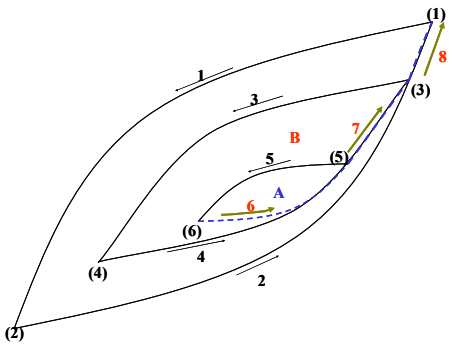

Fig. 3 Reversal points in hysteresis trajectories

C. Initialization

Before starting the time loop solution, it is needed to initialize the reversal points stack. The first 2 points of this stack are initialized with very high flux (10^{10} Wb) for defining the borders of the major loop. The remaining variables depend on the type of initialization.

If 'manual' initial conditions (manual remanent flux ϕ_0) are used then the initialization proceeds as shown in Fig. 4. Point 2 (current i_2) is arbitrarily chosen for a current 50 times the coercive current. The next step is to determine equation (2) for a trajectory passing through ϕ_0 which will give point 1. It is assumed that the trajectory between the last reversal point and ϕ_0 is a downward trajectory if $\phi_0 \geq 0$ and upward trajectory if $\phi_0 < 0$. Such behavior is consistent with the deenergization pattern of a transformer. The point 2 is chosen sufficiently high to enable placing ϕ_0 on the upper trajectory between 2 and 1 when $\phi_0 \geq 0$ and on the lower trajectory when $\phi_0 < 0$. If this condition is not satisfied then point 2 must be moved. The same technique is applicable to $\phi_0 = 0$.

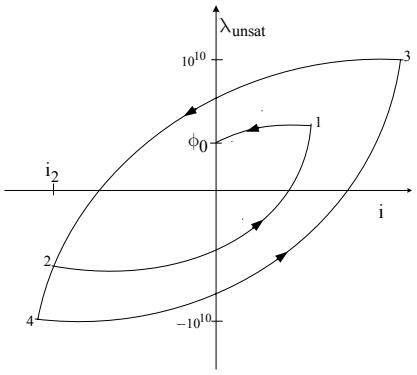

Fig. 4 Reversal points stack for manual initial conditions

If it is chosen to connect the reactor during the steady-state phasor solution, one option is to use an inductance value taken from the slope of the major hysteresis loop at zero flux. In this case the initialization points are given in Fig. 5. Points 3 and 4 are defined using $10\phi_{ss}$. The choice of $10\phi_{ss}$ (where ϕ_{ss} is the flux at t=0 from the steady-state phasor solution) is again arbitrary, but has been found acceptable in most cases.

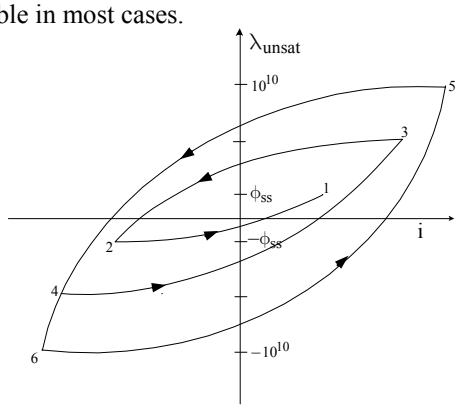

Fig. 5 Reversal points stack initialization from steady-state

IV. Implementation in EMTP

A. The fitter

As a first step it is required to provide a fitting method for determining the parameters of equations (1) and (2). The new fitter uses a least-squares method for finding the saturation function parameters of equation (1). The parameter S_{hv} of equation (2) is also determined by this method since during the fitting process λ_{unsat} is replaced by $S_{hv}i$. The remaining parameters of equation (2) are determined from minor loop data. The coercive current is determined from the major loop data or can be entered manually when only a centered raw data is available. The user is allowed to visualize the fitting results and improve them by manipulating parameters.

Fig. 6 compares a case of raw data with fitted data. The requisite symmetry of the hyperbolic curves complicates the fitting if the available characteristic has a lack of symmetry. It also noticed that the fitting could have been improved if 3rd or 4th order equations were used instead of the quadratic model of equation (1).

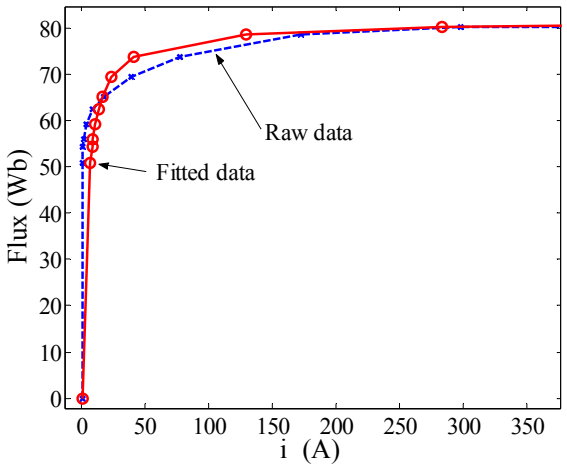

Fig. 6 Fitting example

B. Equivalent circuit

The new hysteretic reactor has been implemented into a new EMTP code, named EMTP-RV [11][12]. To allow a completely general solution where nonlinear model functions can be solved without topological restrictions, EMTP-RV uses an iterative setup with the entire system of linear equations. Nonlinear devices are required to simply return their discretized Norton equivalent through linearization at the given operating point for time-point t. This constitutes a Newton method.

The topological restrictions due to the compensation method are eliminated, since there is no need to calculate a Thevenin network equivalent as seen by the reactor. Thevenin impedance or admittance conditioning problems [9] are avoided. Since there is no separation between the linear and nonlinear network (see [9] for details) solutions

and all nonlinear functions are always present, there are no restrictions on mixing nonlinear functions of various types. Contrary to the previous type-92 model, one can place the nonlinear hysteretic reactor in parallel with a nonlinear arrester model or use several combinations of nonlinear reactors without restrictions on voltage loops [9].

In EMTP-RV, the hysteretic reactor is a flux-input/current-output element. At each solution time-point it is converted into the Norton equivalent shown in Fig. 7. This is similar to the nonlinear inductance model. The flux $\phi_t^{(j)}$ (at time-point t and iteration j) is first found from the network voltage $v_t^{(j)}$ using the trapezoidal integration method with time-step Δt :

$$\phi_t^{(j)} = \frac{\Delta t}{2} v_t^{(j)} + \phi_{history} \tag{3}$$

This flux is entered into equation (1) as λ_{sat} to find λ_{unsat} and then into equation (2) to find the current on the undertaken trajectory and $\phi_{q_t}^{(j)}$ (ordinate at the origin of the operating segment) in:

$$\phi_t^{(j)} = K_{q_t}^{(j)} i_t + \phi_{q_t}^{(j)} \tag{4}$$

The calculation of $K_{q_t}^{(j)}$ requires the differentiation of both (1) and (2):

$$K_{q_t}^{(j)} = \left.\frac{\partial \phi}{\partial \lambda_{unsat}}\right|_{\phi_t^{(j)}, \lambda_{unsat_t}^{(j)}} \left.\frac{\partial \lambda_{unsat}}{\partial i}\right|_{\lambda_{unsat_t}^{(j)}, i_t^{(j)}} \tag{5}$$

It can be shown that the combination of (3) and (4) results into:

$$i_t = \frac{\Delta t}{2K_{q_t}^{(j)}} v_t + \frac{1}{K_{q_t}^{(j)}} \left(\phi_{history} - \phi_{q_t}^{(j)} \right) \tag{6}$$

which corresponds to the circuit of Fig. 7.

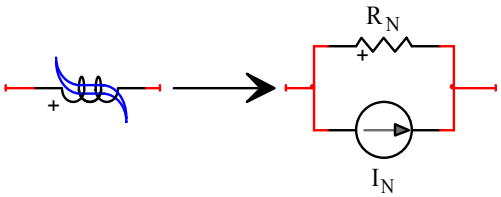

Fig. 7 Hysteretic reactor equivalent circuit

This new approach has a fast convergence attribute by achieving the best available prediction for next time-point due to the linear solution movement with the nonlinear function of the reactor.

V. TEST CASE

A high-level view (does not show all details, one-line diagram with subnetworks) of the selected test case is shown in Fig. 8. The test case studies the energization of a set of two interconnected target transformers (three-pole 3x360 MVA and three-phase 2x29 MVA) when a second 600 MVA transformer has been already energized through a long line. The generator at the sending end is a 900 MW machine, which is modeled as an ideal source behind its subtransient reactance. The long line and the interconnecting cables are modeled using pi-sections. The detailed case includes a total of 5 transformers: an autotransformer at the receiving end of the line, the step-up transformer at the source end, the load transformer at the source end, the step-down target transformer and the second load transformer at the target. The target transformers (target is used here to denote the energized transformers) are modeled using the hysteretic reactor model presented in this paper. This approach allows to account for remanent flux at energization. All other transformers contain a nonlinear inductance. All nonlinear models are solved simultaneously with the linear network using the techniques developed in EMTP-RV [11].

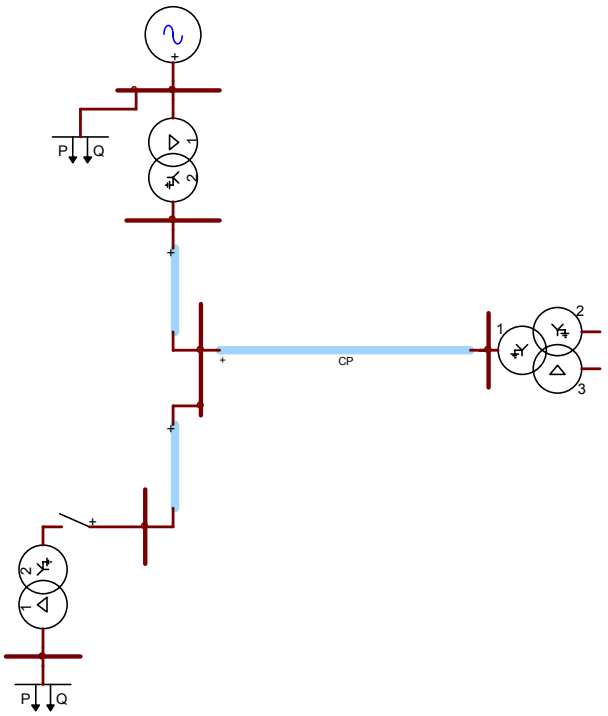

Fig. 8 Simulated case

This case as assembled, could not be solved using previously available EMTP methods [1]. In addition to the fact that the previously programmed compensation technique did not allow mixed nonlinear functions, both the type-92 and type-96 hysteretic models were unable to achieve convergence.

The breaker shown in Fig. 8 is initially closed to establish steady-state conditions. It is then opened at 10 ms and reclosed again at 1.7 s. Fig. 9 shows the phase-a voltage at the breaker. The red line (solid line) is using the hysteretic reactor model, while the blue (dotted line) shows the same simulation when a simple nonlinear inductance is used to model saturation. It is apparent that due to its ability to maintain remanent flux, the hysteretic reactor is allowing to observe an overvoltage of approximately 1.7 pu.

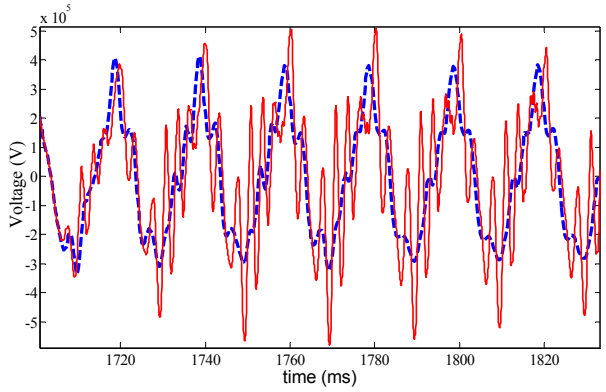

Fig. 9 Energization of target transformers, phase-a voltage at the breaker

Fig. 10 presents a view of hysteresis trajectories for phase-a of the first target transformer. The reactor is on a steady-state trajectory before the occurrence of the transient that moves on the minor loops.

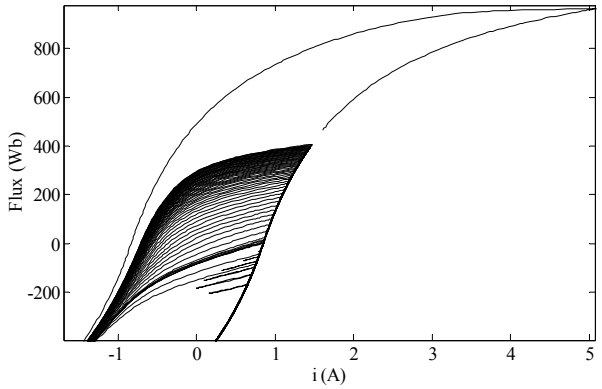

Fig. 10 Hysteresis trajectories for phase-a of reenergized target transformer

It is valuable to mention that the mean number of iterations per time-point is about 2.21 and the total CPU time is 60 s for a simulation interval of 3 s using $\Delta t = 50\mu s$ on a Pentium-4 computer of 1.7 GHz. The complete network contains a total of 200 nodes and 250 devices. The simulation time is dramatically reduced by the ability of the setup to achieve steady-state conditions at simulation startup.

VI. Conclusions

This paper has presented the implementation of a new hysteretic reactor model for transient analysis. The model has been demonstrated using the EMTP-RV environment. The physical model as such, has been derived from previously available work, but its numerical solution and implementation are new. Important problems, such as initialization, fitting and integration into a Newton solution have been presented. The model has been used in a practical test case of transformer energization. The test case solution has achieved new and not previously available simulation capabilities.

VII. References

[1] Electromagnetic Transients Program (EMTP), EMTP-V3, Development Coordination Group of EMTP.

[2] A. Narang, E. P. Dick, R. C. Cheung “Transformer Model for ElectroMagnetic Transient Studies”, CEA Report 175 T 331 G, December 1996.

[3] E. P. Dick and W. Watson, “Transformer Models for Transient Studies Based on field Measurements”, IEEE Transactions on Power Apparatus and Systems, Vol. PAS-100, No. 1, January 1981, pp. 409-419.

[4] S. N. Talukdar and J. R. Bailey, “Hysteresis Model for System Studies” IEEE Transactions on Power Apparatus and Systems, Vol. PAS-95, July/August 1976, pp. 1429-1434.

[5] J. G. Frame, N. Mohan, T. Liu, “Hysteresis Modeling in an Electromagnetic Transients Program”, IEEE Transactions, Vol PAS-101, No. 9, Sept. 1982, pp. 3403-3412.

[6] D. N. Ewart, “Digital Computer Simulation Model of a Steel-Core Transformer”, IEEE, Transactions on Power Delivery, Vol. PWRD-1, No. 3, July 1986, pp. 174-183.

[7] A. Wright, A. and Carneiro Jr., S. - "Analysis of Circuits Containing Components with Cores of Ferromagnetic Material" - Proceedings IEE, Vol 121, n 12, December 1974, pp. 1579-1581.

[8] H. W. Dommel, “Nonlinear and time-varying elements in digital simulation of electromagnetic transients”, IEEE Transactions, Vol. PAS-90, 1971, pp. 2561-2567

[9] J. Mahseredjian, S. Lefebvre and X.-D. Do : “A new method for time-domain modeling of nonlinear circuits in large linear networks”. 11th Power Systems Computation conference (PSCC), Proceedings Vol. 2, August 1993, pp. 915-922.

[10] A. Semlyen and A. Castro : “A digital transformer model for switching transient calculations in three phase systems”, PICA Conference Proceedings, New Orleans, June 1975, pp. 121-126

[11] J. Mahseredjian, L. Dubé, L. Gérin-Lajoie, “New advances in the Simulation of Transients with EMTP: Computation and Visualization Techniques”, Electrimacs, August 19th, 2002, Plenary session paper.

[12] J. Mahseredjian, “EMTPWorks, a graphical user interface for EMTP”, Hydro-Québec, 2002